Journal of Materials Chemistry C

COMMUNICATION

View Article Online
View Journal | View Issue

Cite this: J. Mater. Chem. C, 2019, 7, 13047

Received 12th August 2019,
Accepted 4th October 2019

DOI: 10.1039/c9tc04459k

rsc.li/materials-c

Triphenylpyrazine: methyl substitution to achieve deep blue AIE emitters†

Haozhong Wu,[a] Jiajie Zeng,[a] Zeng Xu,[a] Bing Zhang,[a] Han Zhang,[a] Yuyu Pan,[b] Zhiming Wang,*[ab] Dongge Ma,[a] Anjun Qin[a] and Ben Zhong Tang*[ac]

Based on our deep comprehension of the unique excited state decay process of tetraphenylpyrazine derivatives, triphenylpyrazine-3-carbazole (TrPP-3C) was designed by replacing the phenyl group with a methyl group at the 3-position of pyrazine. Compared to the values for its model tetraphenylpyrazine-3-carbazole (TPP-3C), the Commission International de l'Eclairage (CIE) coordinates of TrPP-3C shifted to the more valuable deep-blue region in the non-doped device, demonstrating that the in-depth study of the excited state distribution was of great significance for the development of a new aggregation-induced emission (AIE) building block.

Organic light-emitting diodes (OLEDs) have attracted continuously increasing attention in the last three decades and are deemed to be the most promising candidates for the new-generation full-color, large-area, flat-plane and flexible displays. Up to now, blue, green and red OLEDs have performed well and satisfied the requirements for practical applications.[1–9] Nevertheless, high-efficiency deep blue OLEDs with CIE coordinates ($x + y < 0.3$) are still limited; thus, this has been an ongoing challenge that has triggered wide-ranging efforts for its resolution.[10–13]

Generally, rigid planar structures with finite conjugation are fundamental for deep blue luminescent materials owing to their low conformational relaxation, which can achieve narrow full width at half maximum (FWHM) to improve the colour purity. However, these dyes, *e.g.*, anthracene and pyrene often generate weak fluorescence with red-shifted emission in the aggregate form due to the undesirable strong interaction in their stacking situation.[14–17] To avoid these adverse factors, some fluorophores have been constructed with aggregation-induced emission luminogens (AIEgens), such as tetraphenylethene (TPE), because most of them have relatively twisted structures that can prevent H-aggregation and π–π stacking. However, the TPE-based luminophores usually show fluorescence with broad FWHM and are not suitable for achieving outstanding deep blue emission because of the numerous flexible conformations in their aggregates.[11,18–21] Therefore, we have to divert our attention to search for other AIEgens that are suitable for achieving deep blue emission. Tetraphenylpyrazine (TPP) is a good AIE building block previously reported by our group, and it emits violet-blue fluorescence with an emission peak at 390 nm and acceptable FWHM in films.[22] Besides, some TPP-based compounds with blue emission have been developed with a good performance in non-doped OLEDs, but it is still difficult to obtain high-quality deep blue emitters.[23–25]

Recently, we discovered that their transition process was chiefly determined by the conjugation along the substituted axis direction, while the two off-axis phenyl groups seemed to have a negligible effect on their emission. However, the detailed analysis of the frontier orbital distribution for 9-(4-(3,5,6-triphenylpyrazin-2-yl)phenyl)-9*H*-carbazole and 9-(4′-(3,5,6-triphenylpyrazin-2-yl)-[1,1′-biphenyl]-4-yl)-9*H*-carbazole (TPP-PhCz) showed that the phenyl group at the 3-position in pyrazine participated in the transition process to some extent.[24] This might significantly affect the OLED performance of the TPP derivatives after substitution occurs there. Herein, **TPP-3C** and **TrPP-3C** (triphenylpyrazine, TrPP) were designed to determine the feasibility of replacing the phenyl ring with a non-conjugative methyl group to achieve deep-blue emitters, while 3-carbazole was inserted instead of 9-phenyl-carbazole in TPP-PhCz for enhancing the luminescence efficiency (Fig. 1A).

To demonstrate our strategy, a theoretical calculation was employed first. The geometries of **TrPP-3C** and **TPP-3C** in the S_0 and S_1 states were optimized using the density functional

[a] State Key Laboratory of Luminescent Materials and Devices, Center for Aggregation-Induced Emission, Key Laboratory of Luminescence from Molecular Aggregates of Guangdong Province, Guangzhou International Campus, South China University of Technology (SCUT), Guangzhou 510640, China. E-mail: wangzhiming@scut.edu.cn

[b] School of Petrochemical Engineering, Shenyang University of Technology (SUT), Liaoyang 111003, China

[c] Department of Chemistry, The Hong Kong University of Science & Technology (HKUST), Clear Water Bay, Kowloon, Hong Kong, China. E-mail: tangbenz@ust.hk

† Electronic supplementary information (ESI) available: NMR spectra for target compounds, photophysical properties, thermogravimetric and differential scanning calorimetry curve, cyclic voltammetry. See DOI: 10.1039/c9tc04459k

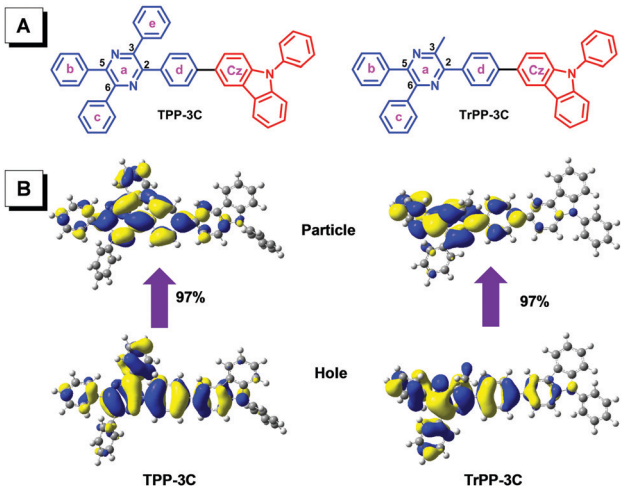

Fig. 1 (A) The molecular structures and optimized geometries of two compounds in the S_1 states; (B) natural transition orbitals of **TPP-3C** and **TrPP-3C** in the S_1 states.

theory (DFT) and time-dependent density functional theory (TD-DFT) with the M06-2X/6-31G(d,p) level on the Gaussian 09 program.[26] As shown in Fig. S1 (ESI†), the highest occupied molecular orbitals (HOMOs) are mostly present on carbazole and the adjacent phenyl groups, while the lowest unoccupied molecular orbitals (LUMOs) are localized on the TrPP or TPP group, which indicates that the separated HOMO/LUMO distributions have significant intramolecular charge transfer (ICT) characteristics in the S_0 states for the two compounds. However, the situation changed obviously in the excited states, as shown in Fig. 1B and Table S1 (ESI†). For example, the dihedral angles α_{a-d} and α_{a-e} became smaller in the excited states (−38.34 and 16.26° for **TPP-3C**; −13.56 and −11.40° for **TrPP-3C**) than those in the ground states (−41.34 and 41.49° for **TPP-3C**; −36.29 and −33.41° for **TrPP-3C**). This suggested that the TPP and TrPP units underwent a planarization process upon excitation as we previously reported.[24,25] After the planarization of the molecular conformations, both holes and particles were dispersed on the TrPP or TPP and adjacent phenyl groups (carbazole moieties); this implied that the S_1 states were local excited states and were generally in favour of fluorescing for both compounds. Besides, the dihedral angle between the TrPP unit and 3-carbazole of **TrPP-3C** (32°) was larger than that of **TPP-3C** (24°) in their excited states, suggesting the limited conjugation along the substituted axis in the **TrPP-3C**'s excited state; thus, **TrPP-3C** might exhibit bluer emission in solution and in the film state because of some larger distortion angle in its main transition direction compared to **TPP-3C**.

For a better description of our design, the transition density matrix of **TPP-3C** and **TrPP-3C** was then calculated on Multiwfn to explore the effect of each moiety on the radiative decay behaviour.[27–29] As shown in Fig. 2, the brightness and red-shifted colour (value) of the blocks exhibit a positive correlation with the involvement of the $S_1 \rightarrow S_0$ transition on the sub-units. The dotted blocks on diagonal (a,a), (b,b), (c,c), (d,d), (e,e) and (Cz,Cz) usually represent the transition of the local excited state when the off-diagonal blocks such as (a,b) and (a,d) are considered to be the transition with some CT feature. First, the values of the dotted blocks (a,a) were the highest among all the blocks and most of the blocks related to the a group, *e.g.*, (a,X)/(X,a) [X = b, d, e, Cz] were also bright for both **TPP-3C** and **TrPP-3C**, implying that the a (pyrazine) ring played a key role in the radiation transition process of **TPP-3C** and **TrPP-3C**. The values of blocks (d,d) and (a,d)/(d,a) also indicated relatively large intensities, suggesting that the d phenyl group was also important for the $S_1 \rightarrow S_0$ transition of the two molecules. From the careful observation of Fig. 2, we can distinguish their transition difference. In the off-axis substituted direction of **TPP-3C**, the block (c,c) was darker than the block (e,e), which demonstrated that the transition participation of the c phenyl group was far less than that of the e phenyl group in **TPP-3C**. Therefore, it would be meaningful to perform substitution on the e phenyl group instead of the c position. Before the methyl group replacement, the values of (b,b) and (a,b)/(b,a) were

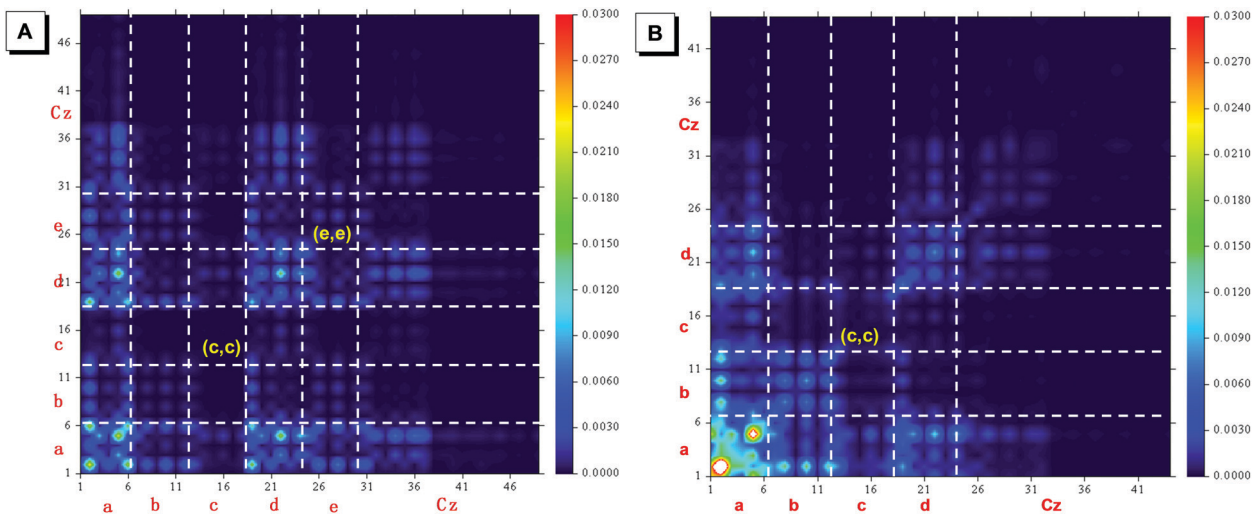

Fig. 2 The transition density matrix of **TPP-3C** (A) and **TrPP-3C** (B).

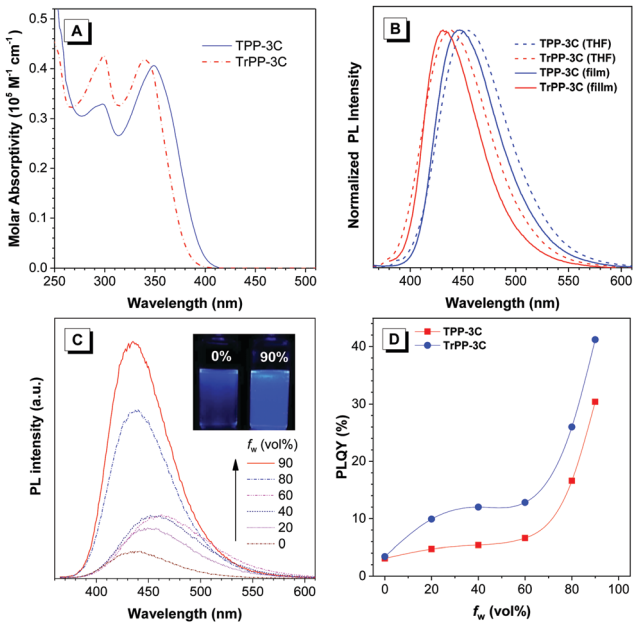

Fig. 3 (A) The absorption spectra of **TPP-3C** and **TrPP-3C** in THF solution. (B) The normalized PL spectra of **TPP-3C** and **TrPP-3C** in THF solution and film (concentration: 10^{-5} M). (C) The PL spectra of **TrPP-3C** in THF/water mixtures with different water fractions; concentration: 10^{-5} M. Inset: Photos of the compounds in THF/water mixtures (f_w = 0 and 90%) taken under 365 nm excitation. (D) The plots of PLQY as a function of different water fractions (f_w) in THF/H_2O mixtures for **TrPP-3C** and **TPP-3C** (concentration: 10^{-5} M).

relatively weak in **TPP-3C**. After replacement, these intensities were enhanced in **TrPP-3C**, which testified that the b phenyl group of **TrPP-3C** was more involved in the transition process, and these changes were caused by methyl substitution at the 3-position of pyrazine. Furthermore, the integral intensity of the transition density matrix increased significantly in **TrPP-3C**, which would be conducive to the improvement in the photoluminescence efficiency. Hence, we believed that **TrPP-3C** would exhibit effective deep-blue emission as expected. In addition, these relatively bright transition blocks of $S_1 \rightarrow S_0$, such as (a,X)/(X,a), (d,X)/(X,d) and (Cz,X)/(X,Cz) ([X = a, d, Cz] either with LE or CT states), were mainly distributed along the substituted direction, which is consistent with the excited-state quinone-conformation induced planarization process on TPP-based derivatives.[25]

Based on the above theoretical analysis, the two compounds were prepared following the synthesis route shown in Fig. S2 (ESI†), and their structures were confirmed *via* nuclear magnetic resonance spectroscopy and high-resolution mass spectroscopy (Fig. S3–S11, ESI†). The photophysical properties of **TrPP-3C** and **TPP-3C** were analysed based on the absorption spectra and photoluminescence (PL) spectra. As depicted in Fig. 3A, **TrPP-3C** and **TPP-3C** exhibit strong absorptive peaks at 340 nm and 349 nm in THF solutions, respectively, which can be assigned to the π–π* transition. The blue-shifted absorptive profile of **TrPP-3C** suggested that the TrPP-based derivative possessed short conjugation in contrast to the TPP-based one, as calculated above. Similarly, **TrPP-3C** (437 nm in THF and 432 nm in film) displayed 17 and 15 nm blue-shifted emissions compared with **TPP-3C** (454 nm in THF and 447 nm in film) in the THF solution and film state, respectively (Fig. 3B and Table 1), demonstrating that **TrPP-3C** was more suitable as a deep blue luminogen than **TPP-3C** as the calculation predicted. As shown in Table 1, **TrPP-3C** and **TPP-3C** emitted strongly with higher quantum yields (Φ) of 47.2% and 36.6% in the film state than 3.9% and 3.0% in THF solutions, respectively, indicating their AIE features.

To confirm this point, the PL intensities of **TrPP-3C** and **TPP-3C** were investigated in THF/water mixtures with different water fractions (f_w). As displayed in Fig. 3C and D, the PL intensity of **TrPP-3C** increases slowly before f_w = 60% (unaggregated), while a drastic improvement in the PL intensity is observed once f_w > 60% due to the formation of aggregates. This suggested that structure modification did not affect the

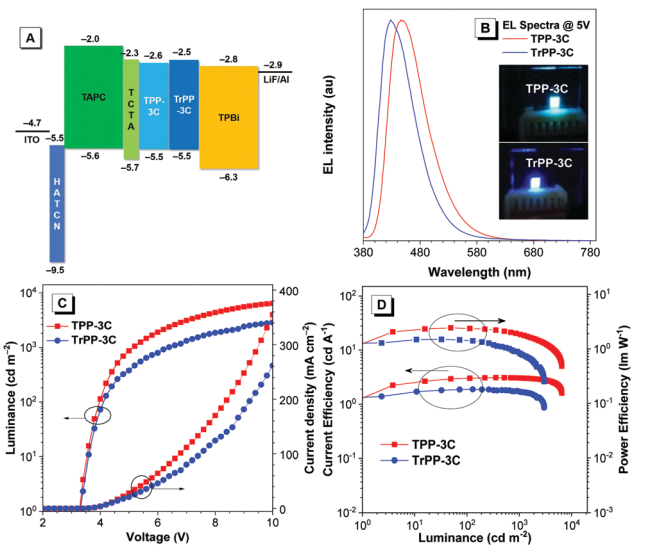

Fig. 4 (A) The energy diagram of the device structure; (B) EL spectra at 5 V; (C) current density–voltage–luminescence, and (D) current efficiency–luminescence–power efficiency characteristics of **TPP-3C** and **TrPP-3C**. Inset: Photos of OLEDs based on **TPP-3C** and **TrPP-3C**.

Table 1 The photophysical properties of **TPP-3C** and **TrPP-3C**

Compound	λ_{abs}[a] (nm)	λ_{em}[b] (nm)		Φ[c] (%)		τ[d] (ns)		K_r[e] (10^7 s^{-1})		K_{nr}[f] (10^7 s^{-1})	
		Soln	Film	Soln	Film	Soln	Film	Soln	Film	Soln	Film
TPP-3C	349	454	447	3.0	36.6	0.40	0.91	7.5	40.2	242.5	69.7
TrPP-3C	340	437	432	3.9	47.2	0.52	1.67	7.5	28.1	184.8	31.6

[a] Maximum absorption wavelength, concentration: 10 μM. [b] Maximum emission wavelength, soln: THF solution, film: droplet film. [c] Absolute fluorescence quantum efficiency. [d] Luminescence lifetime. [e] $K_r = \Phi/\tau$. [f] $K_{nr} = (1 - \Phi)/\tau$.

Table 2 The electroluminescence performance of the devices

		Maximum values				Values at 1000 cd m^{-2}				
Device	V_{on}[a] (V)	η_C[b] (cd A^{-1})	η_P[b] (lm W^{-1})	EQE[b] (%)	L[b] (cd m^{-2})	η_C[b] (cd A^{-1})	η_P[b] (lm W^{-1})	EQE[b] (%)	CIE(x, y)[c]	λ_{EL}[d] (nm)
TPP-3C	3.3	3.09	2.43	2.81	6527	3.03	1.83	2.76	(0.150, 0.145)	444
TrPP-3C	3.3	1.88	1.49	2.89	2995	1.71	0.84	2.62	(0.152, 0.086)	428

[a] V_{on} = turn-on voltage at 1 cd m^{-2}. [b] η_C = current efficiency; η_P = power efficiency; EQE = external quantum efficiency; L = luminance. [c] CIE = Commission International de I'Eclairage coordinates at 10 mA cm^{-2} current density. [d] λ_{EL} = maxima of electroluminescence spectra.

AIE feature, and TrPP would become a promising deep-blue AIEgen. Similar to most TPP derivatives, **TPP-3C** also exhibited a perfect AIE plot (Fig. S12, ESI†). In addition, gradually red-shifted PL profiles appeared as the water fractions increased up to 60% due to the ICT states, which were verified by the solvatochromism investigation in different-polarity solvents (Fig. S13 and Table S2, ESI†). When in the aggregated state, the PL emission shifted to the blue region because the environment polarity was smaller in the nanoparticle states than in THF/water solutions (f_w < 60%).[30] Besides, their luminescence lifetimes were of the order of nanoseconds with one component, which referred to the normal fluorescence emission (Fig. S14, ESI†). Similar to the observations for previous TPP-based derivatives, increase in the radiative decay rates (K_r) in **TrPP-3C** was observed, which might originate from its planar conformation in the excited states, and this conjecture was consistent with the above theoretical calculation and our reported results.[24] Meanwhile, the decrease in non-radiative decay (K_{nr}) from the THF solution to the film state for **TrPP-3C** also implied that the restriction of the intramolecular motion contributed significantly to the fluorescence enhancement in the aggregate states.[31] The results showed that we obtained a novel deep-blue AIE building block *via* the deep comprehension of the unique excited state on the TPP unit.

For fabricating into OLED devices with a good performance, their thermal properties were measured by thermogravimetric analysis and differential scanning calorimetry under a nitrogen atmosphere. They exhibited good thermal stability with 5% weight loss (T_d) at the temperatures of more than 400 °C as well as good morphological stability with adequate glass-transition temperatures (T_g) of more than 100 °C (Fig. S15, ESI†). The energy levels of HOMOs and LUMOs were estimated from cyclic voltammetry measurements. Similar to their theoretical calculations in the ground state, the two compounds had almost identical HOMO level values (−5.54 eV for **TrPP-3C** and −5.53 eV for **TPP-3C**) because of their electron location on the Cz-dominant group, while the LUMO level values exhibited some differences originating from the absence of the phenyl ring (−2.48 eV for **TrPP-3C** and −2.59 eV for **TPP-3C**) (Fig. S16 and Table S3, ESI†). These results indicate that the compounds were appropriate for OLED emitters.

Non-doped OLED devices were fabricated with the device configuration of ITO/HATCN (5 nm)/TAPC (40 nm)/TCTA (5 nm)/**TrPP-3C** or **TPP-3C** (20 nm)/TPBi (40 nm)/LiF (1 nm)/Al. In the devices, HATCN (2,3,6,7,10,11-hexacyano-1,4,5,8,9,12-hexaazatriphenylene) and TAPC (1,1-bis[4-[*N*,*N*-di(*p*-tolyl)amino]-phenyl]cyclohexane) served as the hole-injecting layer and hole-transporting layer, respectively. TCTA (4,4′,4″-tri-9-carbazolytriphenylamine) functioned as the hole-transporting layer and electron-blocking layer. TPBi (2,2′2″-(1,3,5-benzinetriyl)tris-(1-phenyl-1-*H*-benzimidazole)) was used as the electron-transporting layer and hole-blocking layer (Fig. 4A). The key data and characteristic curves are given in Table 2 and Fig. 4. The devices were turned on at a low voltage of 3.3 V for both compounds. **TrPP-3C** exhibited deep blue electroluminescence emission with a peak (λ_{EL}) at 428 nm and CIE coordinates of (0.152, 0.086). It also achieved good external quantum efficiency (EQE) of 2.89%, η_C of 1.88 cd A^{-1} and η_P of 1.49 lm W^{-1}. Compared to the **TPP-3C**-based OLED with EQE of 2.81% and CIE coordinates of (0.150, 0.145), the **TrPP-3C**-based device did not exhibit improvement in efficiency, but its CIE coordinates blue-shifted to a more valuable area, which proved that this structural modification of converting a phenyl group into a non-conjugative methyl group on polyphenylpyrazine seemed to be successful. Besides, the performance of **TrPP-3C** was much better than that of most reported AIEgens with deep blue emission, as shown in Table S4 (ESI†).

In summary, we found that four phenyl substituents had different effects on the transition process of the TPP derivatives *via* a deep understanding of the unique excited state. The S_1 to S_0 transition process originated primarily from the conjugation along the substituted axis, while in the off-axis direction, the e phenyl group (at the 3-position of pyrazine) also participated to some extent based on systematic theoretical analysis. Thus, the non-conjugated methyl group in **TrPP-3C** was employed to replace this phenyl group on **TPP-3C**, and a novel deep-blue AIE emitter was obtained. In non-doped OLEDs, **TrPP-3C** displayed a better device performance with appreciable maximum EQE of 2.89% and desirable CIE coordinates of (0.152, 0.086) compared with **TPP-3C**. All these results indicate that the strategy of confining conjugation on the 3-position substitution group of pyrazine is essential to develop high-efficiency deep blue emitters based on the TPP group. Therefore, the profound investigation of the excited state changes will be of great significance for the development of new AIE building blocks.

Conflicts of interest

There are no conflicts to declare.

Acknowledgements

This work is financially supported by National Natural Science Foundation of China (21788102, 51673118 and 21975077), Science & Technology Program of Guangzhou (201804010218

and 201804020027), Science and Technology Plan of Shenzhen (JCYJ20160428150429072 and JCYJ20160229205601482), the Innovation and Technology Commission of Hong Kong (ITC-CNERC14S01), the Fundamental Research Funds for the Central Universities (D2190960) and Fund of Key Laboratory of Luminescence from Molecular Aggregates of Guangdong Province (2019B030301003).

Notes and references

1 C.-H. Chang, Z.-J. Wu, C.-H. Chiu, Y.-H. Liang, Y.-S. Tsai, J.-L. Liao, Y. Chi, H.-Y. Hsieh, T.-Y. Kuo, G.-H. Lee, G.-H. Pan, P.-T. Chou, J.-S. Lin and M.-R. Tseng, *ACS Appl. Mater. Interfaces*, 2013, **5**, 7341–7351.
2 H. Shin, J. H. Lee, C. K. Moon, J. S. Huh, B. Sim and J. J. Kim, *Adv. Mater.*, 2016, **28**, 4920–4925.
3 Y.-C. Zhu, L. Zhou, H.-Y. Li, Q.-L. Xu, M.-Y. Teng, Y.-X. Zheng, J.-L. Zuo, H.-J. Zhang and X.-Z. You, *Adv. Mater.*, 2011, **23**, 4041–4046.
4 C.-H. Chang, M.-C. Kuo, W.-C. Lin, Y.-T. Chen, K.-T. Wong, S.-H. Chou, E. Mondal, R. C. Kwong, S. Xia, T. Nakagawa and C. Adachi, *J. Mater. Chem.*, 2012, **22**, 3832–3838.
5 H. Sasabe, Y. Seino, M. Kimura and J. Kido, *Chem. Mater.*, 2012, **24**, 1404–1406.
6 Y. Seino, S. Inomata, H. Sasabe, Y. J. Pu and J. Kido, *Adv. Mater.*, 2016, **28**, 2651.
7 C. Li, R. Duan, B. Liang, G. Han, S. Wang, K. Ye, Y. Liu, Y. Yi and Y. Wang, *Angew. Chem., Int. Ed.*, 2017, **56**, 11525–11529.
8 T. Liu, L. Zhu, S. Gong, C. Zhong, G. Xie, E. Mao, J. Fang, D. Ma and C. Yang, *Adv. Opt. Mater.*, 2017, **5**, 1700145.
9 W. W. H. Lee, Z. Zhao, Y. Cai, Z. Xu, Y. Yu, Y. Xiong, R. T. K. Kwok, Y. Chen, N. L. C. Leung, D. Ma, J. W. Y. Lam and B. Z. Tang, *Chem. Sci.*, 2018, **9**, 6118–6125.
10 Y. Zhang, S.-L. Lai, Q.-X. Tong, M.-F. Lo, T.-W. Ng, M.-Y. Chan, Z.-C. Wen, J. He, K.-S. Jeff, X.-L. Tang, W.-M. Liu, C.-C. Ko, P.-F. Wang and C.-S. Lee, *Chem. Mater.*, 2012, **24**, 61–70.
11 Q. Li and Z. Li, *Adv. Sci.*, 2017, **4**, 1600484.
12 Y. Yu, Z. Wu, Z. Li, J. Bo, L. Li, L. Ma, D. Wang, G. Zhou and X. Hou, *J. Mater. Chem. C*, 2013, **1**, 8117–8127.
13 S. Chen, J. Lian, W. Wang, Y. Jiang, X. Wang, S. Chen, P. Zeng and Z. Peng, *J. Mater. Chem. C*, 2018, **6**, 9363–9373.
14 H. Park, J. Lee, I. Kang, H. Y. Chu, J.-I. Lee, S.-K. Kwon and Y.-H. Kim, *J. Mater. Chem.*, 2012, **22**, 2695–2700.
15 C. Dennis, S.-J. Yoo, M. Baumgarten, J.-J. Kim and K. Müllen, *J. Mater. Chem. C*, 2014, **2**, 9083–9086.
16 W. Sun, N. Zhou, Y. Xiao, S. Wang and X. Li, *Chem. – Asian J.*, 2017, **12**, 3069–3076.
17 W. Sun, N. Zhou, Y. Xiao, S. Wang and X. Li, *Dyes Pigm.*, 2018, **154**, 30–37.
18 J. Huang, R. Tang, T. Zhang, Q. Li, G. Yu, S. Xie, Y. Liu, S. Ye, J. Qin and Z. Li, *Chem. – Eur. J.*, 2014, **20**, 5317–5326.
19 W. Qin, Z. Yang, Y. Jiang, J. W. Y. Lam, G. Liang, H. S. Kwok and B. Z. Tang, *Chem. Mater.*, 2015, **27**, 3892–3901.
20 C. Li, J. Wei, J. Han, Z. Li, X. Song, Z. Zhang, J. Zhang and Y. Wang, *J. Mater. Chem. C*, 2016, **4**, 10120–10129.
21 B. Liu, H. Nie, X. Zhou, S. Hu, D. Luo, D. Gao, J. Zou, M. Xu, L. Wang, Z. Zhao, A. Qin, J. Peng, H. Ning, Y. Cao and B. Z. Tang, *Adv. Funct. Mater.*, 2016, **26**, 776–783.
22 M. Chen, L. Li, H. Nie, J. Tong, L. Yan, B. Xu, J. Z. Sun, W. Tian, Z. Zhao, A. Qin and B. Z. Tang, *Chem. Sci.*, 2015, **6**, 1932–1937.
23 M. Chen, H. Nie, B. Song, L. Li, J. Z. Sun, A. Qin and B. Z. Tang, *J. Mater. Chem. C*, 2016, **4**, 2901–2908.
24 L. Pan, H. Wu, J. Liu, K. Xue, W. Luo, P. Chen, Z. Wang, A. Qin and B. Z. Tang, *Adv. Opt. Mater.*, 2019, **7**, 1801673.
25 H. Wu, Y. Pan, J. Zeng, L. Du, W. Luo, H. Zhang, K. Xue, P. Chen, D. L. Phillips, Z. Wang, A. Qin and B. Z. Tang, *Adv. Opt. Mater.*, 2019, 1900283, DOI: 10.1002/adom.201900283.
26 G. W. T. M. J. Frisch, H. B. Schlegel, G. E. Scuseria, J. R. C. M. A. Robb, G. Scalmani, V. Barone, B. Mennucci, H. N. G. A. Petersson, M. Caricato, X. Li, H. P. Hratchian, J. B. A. F. Izmaylov, G. Zheng, J. L. Sonnenberg, M. Hada, K. T. M. Ehara, R. Fukuda, J. Hasegawa, M. Ishida, T. Nakajima, O. K. Y. Honda, H. Nakai, T. Vreven, J. A. Montgomery, Jr., F. O. J. E. Peralta, M. Bearpark, J. J. Heyd, E. Brothers, V. N. S. K. N. Kudin, T. Keith, R. Kobayashi, J. Normand, A. R. K. Raghavachari, J. C. Burant, S. S. Iyengar, J. Tomasi, N. R. M. Cossi, J. M. Millam, M. Klene, J. E. Knox, J. B. Cross, C. A. V. Bakken, J. Jaramillo, R. Gomperts, R. E. Stratmann, A. J. A. O. Yazyev, R. Cammi, C. Pomelli, J. W. Ochterski, K. M. R. L. Martin, V. G. Zakrzewski, G. A. Voth, J. J. D. P. Salvador, S. Dapprich, A. D. Daniels, J. B. F. O. Farkas, J. V. Ortiz, J. Cioslowski and D. J. Fox, *Gaussian 09*, Gaussian, Inc., Wallingford CT, 2013.
27 T. Lu and F. Chen, *J. Comput. Chem.*, 2012, **33**, 580–592.
28 S. Mukhopadhyay, S. P. Jagtap, V. Coropceanu, J.-L. Brédas and D. M. Collard, *Angew. Chem., Int. Ed.*, 2013, **51**, 11629–11632.
29 R. L. Gieseking, S. Mukhopadhyay, C. Risko and J.-L. Brédas, *ACS Photonics*, 2014, **1**, 261–269.
30 J. Huang, N. Sun, P. Chen, R. Tang, Q. Li, D. Ma and Z. Li, *Chem. Commun.*, 2014, **50**, 2136–2138.
31 J. Yang, Z. Chi, W. Zhu, B. Z. Tang and Z. Li, *Sci. China: Chem.*, 2019, **62**, 1090–1098.